Universität Stuttgart

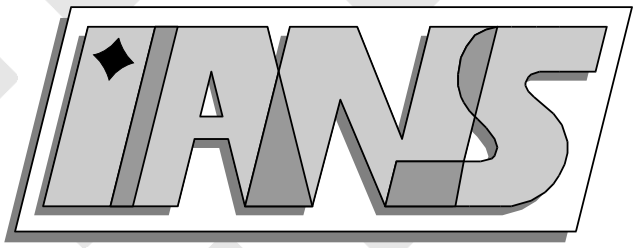

An a posteriori error estimator for the Lamé equation based on $H(\mathrm{div})$-conforming stress approximations

S. Nicaise, K. Witowski, B.I. Wohlmuth

Berichte aus dem Institut für Angewandte Analysis und Numerische Simulation

Preprint 2006/005

Universität Stuttgart

An a posteriori error estimator for the Lamé equation based on $H(\mathrm{div})$-conforming stress approximations

S. Nicaise, K. Witowski, B.I. Wohlmuth

Berichte aus dem Institut für Angewandte Analysis und Numerische Simulation

Preprint 2006/005

Institut für Angewandte Analysis und Numerische Simulation (IANS)
Fakultät Mathematik und Physik
Fachbereich Mathematik
Pfaffenwaldring 57
D-70 569 Stuttgart

E-Mail: ians-preprints@mathematik.uni-stuttgart.de
WWW: http://preprints.ians.uni-stuttgart.de

ISSN **1611-4176**

© Alle Rechte vorbehalten. Nachdruck nur mit Genehmigung des Autors.
IANS-Logo: Andreas Klimke. LaTeX-Style: Winfried Geis, Thomas Merkle.

AN A POSTERIORI ERROR ESTIMATOR FOR THE LAMÉ EQUATION BASED ON $H(\mathrm{DIV})$-CONFORMING STRESS APPROXIMATIONS

S. NICAISE*, K. WITOWSKI†, AND B.I. WOHLMUTH†

Abstract. We derive a new a posteriori error estimator for the Lamé system based on $H(\mathrm{div})$-conforming elements and equilibrated fluxes. It is shown that the estimator gives rise to an upper bound where the constant is one up to higher order terms. The lower bound is also established using Argyris elements. The reliability and efficiency of the proposed estimator is confirmed by some numerical tests.

Key words. equilibrated fluxes, mixed finite elements, a posteriori error estimates, linear elasticity

AMS subject classifications. 65N30, 65N15, 65N50

1. Introduction. The finite element methods are commonly used in the numerical realization of many problems occurring in engineering applications, like the Laplace equation, the Lamé system, the Stokes system, etc.... (see [13, 17]). Adaptive techniques based on a posteriori error estimators have become indispensable tools for such methods. There now exists a large number of publications devoted to the task of analyzing finite element approximations for problems in solid mechanics and obtaining locally defined a posteriori error estimates. We refer to the monographs [2, 10, 29] for a good overview on this topic.

Usually upper and lower bounds are proved in order to guarantee the reliability and the efficiency of the proposed estimator. Most of the existing approaches involve constants depending on the shape regularity of the elements and/or of the jumps in the coefficients; but these dependences are often not given.

For the elasticity system, several different approaches leading to various estimators have been developed (see the review paper [30]). Let us quote the following methods: Residual type error estimators measure the jump of the discrete flux [7, 8, 30]. Another approach is to solve local subproblems by using higher order elements [7, 9, 11, 12]. Very simple and cheap error estimators are the so-called Zienkiewicz-Zhu estimators based on averaging techniques [1, 2, 32, 33]. Finally we can mention estimators based on equilibrated fluxes and on the solution of local Neumann boundary value problems [3, 15, 18, 19, 20, 21, 22, 25, 26, 27, 28].

Here we introduce a locally defined error estimator based on $H(\mathrm{div})$-conforming approximations for the stress and on equilibrated fluxes. In a certain sense in the last described method, we replace the resolution of the local Neumann boundary value problems by explicit $H(\mathrm{div})$-conforming approximations. That renders our estimator more attractive since no supplementary problems have to be solved. This error estimator further yields, up to higher order terms, an upper bound with constant one for the discretization error.

The schedule of the paper is as follows: We recall in Section 2 the boundary value problem and its numerical approximation. Section 3 is devoted to the introduction of the estimator and the proofs of the upper and lower bounds. The upper bound directly follows from the construction of the estimator, while the lower bound requires a specific choice using Argyris elements. In Section 4, we give a practical way to compute explicitly our estimator from the equilibrated fluxes. Finally some numerical tests are presented in Section 5 that confirm the reliability and efficiency of our estimator.

2. The boundary value problem of elasticity and notation. In the context of elasticity, vector- and tensor- or matrix-valued functions will be written in boldface form. The scalar product of two tensors or matrices $\boldsymbol{\sigma}$ and $\boldsymbol{\tau}$ will be denoted by $\boldsymbol{\sigma} : \boldsymbol{\tau}$, and is given by $\boldsymbol{a} : \boldsymbol{b} = a_{ij} b_{ij}$, the summation convention on repeated indices being invoked.

* Université de Valenciennes et du Hainaut Cambrésis, LAMAV, Institut des Sciences et Techniques de Valenciennes, 59313 Valenciennes Cedex 9 France. email: snicaise@univ-valenciennes.fr

†Institute of Applied Analysis and Numerical Simulations (IANS), Universität Stuttgart, Pfaffenwaldring 57, 70529 Stuttgart, Germany. email: {witowski,wohlmuth}@ians.uni-stuttgart.de

This work was supported in part by the Deutsche Forschungsgemeinschaft, SFB 404, B8

Consider a homogeneous isotropic linear elastic material body which occupies a bounded domain Ω in $\mathbb{R}^2$ with Lipschitz boundary Γ. For a prescribed body force $\boldsymbol{f} \in [L^2(\Omega)]^2$, the governing equilibrium equation in Ω reads

$$-\mathrm{div}\boldsymbol{\sigma} = \boldsymbol{f} \ ,$$

where $\boldsymbol{\sigma}$ is the symmetric Cauchy stress tensor. The infinitesimal strain tensor is defined as a function of the displacement $\boldsymbol{u}$ by $\boldsymbol{\epsilon}(\boldsymbol{u}) := \frac{1}{2}(\nabla \boldsymbol{u} + [\nabla \boldsymbol{u}]^\top)$. The displacement is assumed to satisfy the homogeneous Dirichlet boundary condition, i.e., $\boldsymbol{u} = \boldsymbol{0}$ on $\partial\Omega$. With the fourth-order elasticity tensor denoted by $\mathcal{C}$, the constitutive equation reads

$$\boldsymbol{\sigma} = \mathcal{C}\boldsymbol{\epsilon}(\boldsymbol{u}) := \lambda(\mathrm{tr}\,\boldsymbol{\epsilon}(\boldsymbol{u}))\mathbf{1} + 2\mu\,\boldsymbol{\epsilon}(\boldsymbol{u}) \ . \tag{2.1}$$

Here, $\mathbf{1}$ is the identity tensor, and λ and μ are the Lamé parameters, which are constant in view of the assumption of a homogeneous body, and which are assumed positive.

We will make use of the space $L^2(\Omega)$ of square-integrable functions defined on Ω with the inner product and norm being denoted by $(\cdot,\cdot)_0$ and $\|\cdot\|_0$, respectively. The space $H_0^1(\Omega)$ consists of functions in $H^1(\Omega)$ which vanish on the boundary in the sense of traces. For the weak or variational formulations we will require the space $V := [H_0^1(\Omega)]^2$ of displacements; this is a Hilbert space with inner product $(\cdot,\cdot)_1$ and norm $\|\cdot\|_1$ defined in the standard way; that is, $(\boldsymbol{u},\boldsymbol{v})_1 := \sum_{i=1}^2 (u_i, v_i)_1$, with the norm being induced by this inner product. To define our error estimator, we compute by a local postprocessing step an approximation of the symmetric stress $\boldsymbol{\sigma}$. The stress is in $H^{\mathrm{S}}(\mathrm{div};\Omega) := \{\boldsymbol{\tau} \mid \tau_{ji} = \tau_{ij},\ \tau_{ij} \in L^2(\Omega), \mathrm{div}\boldsymbol{\tau} \in [L^2(\Omega)]^2\}$ with the norm $\|\cdot\|_0$ generated in the standard way by the L^2-norm.

Define the bilinear form $a(\cdot,\cdot)$ by

$$a : V \times V \to \mathbb{R}, \qquad a(\boldsymbol{u},\boldsymbol{v}) \quad := \quad \int_\Omega \mathcal{C}\boldsymbol{\epsilon}(\boldsymbol{u}) : \boldsymbol{\epsilon}(\boldsymbol{v})\ dx \ .$$

Associated with the bilinear form is the energy norm $|\!|\!|\boldsymbol{v}|\!|\!|^2 := a(\boldsymbol{v},\boldsymbol{v})$, $\boldsymbol{v} \in V$. Then the standard form of the weak problem for elasticity takes the following form: given $\boldsymbol{f} \in [L^2(\Omega)]^2$, find $\boldsymbol{u} \in V$ that satisfies

$$a(\boldsymbol{u},\boldsymbol{v}) = (\boldsymbol{f},\boldsymbol{v})_0 \ , \quad \boldsymbol{v} \in V \ . \tag{2.2}$$

Let $\mathcal{T}_h$ be a quasi-uniform, shape-regular triangulation of the polygonal domain Ω. We assume that all elements are affine equivalent to the reference triangle $\hat{T}$ with corners $(0,0)$, $(1,0)$ and $(0,1)$ or the reference square $\hat{T} := (-1,1)^2$. The diameter of an element T in $\mathcal{T}_h$ is denoted by h_T. The finite element space $V_h \subset [H_0^1(\Omega)]^2$ for the displacement is taken to be the space of conforming finite elements of lowest order

$$V_h = \{\boldsymbol{v}_h \in [H_0^1(\Omega)]^2 | \quad \boldsymbol{v}_{h|_T} \in V_T, T \in \mathcal{T}_h\},$$

where $V_T := [P_1(T)]^2$ for a triangle and $V_T := [Q_1(\hat{T})]^2 \circ F_T^{-1}$ for a quadrilateral. Here, F_T is the affine mapping from the reference square $\hat{T}$ on T. By $\boldsymbol{u}_h \in V_h$ we denote the finite element solution of the variational problem (2.2), and $\boldsymbol{\sigma}_h$ stands for the elementwise computed discrete stress approximation, i.e., $\boldsymbol{\sigma}_{h|_T} = \mathcal{C}\boldsymbol{\epsilon}(\boldsymbol{u}_{h|_T})$. We note that for both type of elements $\boldsymbol{\sigma}_{h|_T}$ is in $[P_1(T)]^{2\times 2}$, and by definition it is symmetric.

3. Definition of the error estimator. Our error estimator is defined in terms of equilibrated fluxes. Equilibrated fluxes are well established and often used for an adaptive error control, we refer to the monographs [2, 10, 29] and the references therein as well, to the early works [18, 21] and to [26] for a special emphasis on the Lamé equation. A posteriori error estimates for the displacements in terms of local surface tractions are also considered in [15, 19, 25, 27, 28].

For convenience of the reader, we recall the basic ideas. The set of edges of the triangulation is denoted by $\mathcal{E}_h$ and the set of vertices by $\mathcal{P}_h$. With each edge, we associate one unit normal $\boldsymbol{n}_e$, and $\boldsymbol{n}_T$ stands for the outer unit normal of $T \in \mathcal{T}_h$. We note that $\boldsymbol{n}_T$ restricted to the edge e is

equal $\pm\boldsymbol{n}_e$. The orientation of $\boldsymbol{n}_e$ is arbitrary but should be fixed. Then an equilibrated flux is characterized by the following problem: Find for each $e \in \mathcal{E}_h$ a linear function $\boldsymbol{g}_e \in [P_1(e)]^2$ such that the local variational problem is satisfied on each element $T \in \mathcal{T}_h$

$$a_T(\boldsymbol{u}_h, \boldsymbol{v}) = (\boldsymbol{f}, \boldsymbol{v})_{0;T} + \int_{\partial T} \boldsymbol{g}_T \cdot \boldsymbol{v} ds, \quad \boldsymbol{v} \in V_T, \tag{3.1}$$

where $a_T(\cdot,\cdot)$ is the local contribution of the bilinear form $a(\cdot,\cdot)$ restricted to the element T and $\boldsymbol{g}_{T|_e} := \boldsymbol{n}_e \cdot \boldsymbol{n}_T \boldsymbol{g}_e$. Writing $\boldsymbol{g}_e$ as a linear combination of the two nodal basis functions associated with the two endpoints of the edge e, (3.1) yields a global system. However introducing the moments or equivalently biorthogonal basis functions, the global system can be decoupled, and for each vertex $p \in \mathcal{P}_h$, a local system for the moments is obtained, see [2, 21]. The local matrix associated with this linear system is singular for inner vertices and vertices on the Neumann-boundary and has an extremely simple structure. Existence of the solution follows from the fact that $\boldsymbol{u}_h$ is the finite element solution. There are different possibilities to fix the additional degrees of freedoms for the fluxes $\boldsymbol{g}_e$. Basically all approaches are motivated by the observation that for the lower bound of the discretization error, it is crucial to find an equilibrated flux which is as close as possible to the average of the discrete flux; i.e. to $\{\boldsymbol{\sigma}_h \boldsymbol{n}_e\}$. In order to preserve the locality, we do not minimize $\sum_{e\in\mathcal{E}_h} \|\boldsymbol{g}_e - \{\boldsymbol{\sigma}_h \boldsymbol{n}_e\}\|^2_{0;e}$ but minimize the difference between the moments of the equilibrated flux and the average of the discrete flux. We refer to [2] for details regarding the structure of the linear systems, the minimization step and the different cases of vertices associated with the interior of the domain or boundary conditions. To define an equilibrated error estimator, these locally computed fluxes are then used to define local Neumann boundary value problems on each element T. In general, these local Neumann problems are solved numerically by higher order elements, e.g., quadratic elements, and the resulting displacements are used to define the error estimator for which, up to higher order terms, upper and lower bounds in terms of the discretization error can be shown. The influence of the order of the approximation of the Neumann problem is numerically investigated in [10]. We remark that the displacements obtained from the local Neumann problems are in general discontinuous across the elements. Here, we proceed differently. We use the equilibrated fluxes to define locally on each element a $H^{\mathrm{S}}(\mathrm{div};\Omega)$-conforming approximation of the stress. This approximation is then used to define the error estimator yielding the constant one in the upper bound for the error and higher order terms only depending on the data oscillation and being zero if the applied volume force is elementwise linear. Moreover, in many applications the accuracy of the stress is of high importance. Using the hypercycle technique, one can define a new approximation for the stress for which the error estimator is asymptotically exact. For the case of the Laplace operator, we refer to [24], where Raviart–Thomas elements of lowest order are used on a finite volume patch to carry out this idea.

3.1. Upper bounds in terms of mixed finite elements. Unfortunately, there exists no simple low order conforming element for $H^{\mathrm{S}}(\mathrm{div};\Omega)$. Possible remedies are to use macro-elements or to weaken the symmetry condition, see [14]. However if we weaken the symmetry, an additional factor due to the nonconformity of the approach occurs. Therefore, we work with the element proposed in [5] for simplicial triangulations (see also [6]). We refer to [31] for the application of this element to linear elasticity and for the construction of a preconditioner. A $H(\mathrm{div})$-conforming element for quadrilaterals is given in [4]; however, this element yields a local dimension of 45 compared to 31 when using the triangular element on two neighboring triangles, see Lemma 3.1. We therefore cut each quadrilateral into two triangles. If there is a unique shortest diagonal, we use this one as cutting edge e_T, otherwise the choice is arbitrary but should globally be fixed. The new simplicial triangulation is then called $\mathcal{T}_h^{\mathrm{s}}$, and the set of edges being not an element in $\mathcal{E}_h$ is denoted by $\mathcal{E}_h^{\mathrm{n}}$. If $\mathcal{T}_h$ is a simplicial triangulation, we set $\mathcal{T}_h^{\mathrm{s}} := \mathcal{T}_h$ and $\mathcal{E}_h^{\mathrm{n}} = \emptyset$. As before, we denote by $\mathcal{P}_h^{\mathrm{s}}$ and $\mathcal{E}_h^{\mathrm{s}}$ the set of vertices and edges of $\mathcal{T}_h^{\mathrm{s}}$, respectively. By construction, $\mathcal{P}_h^{\mathrm{s}} = \mathcal{P}_h$ and $\mathcal{E}_h^{\mathrm{s}} = \mathcal{E}_h \cup \mathcal{E}_h^{\mathrm{n}}$, and each $T \in \mathcal{T}_h \setminus \mathcal{T}_h^{\mathrm{s}}$ is the union of two elements t_1, $t_2 \in \mathcal{T}_h^{\mathrm{s}}$. We refer to Figure 3.1 for the different sets of edges and the notation. The elements in $\mathcal{E}_h^{\mathrm{n}}$ are indicated by dashed lines in the right picture of Figure 3.1.

The element given in [5] has locally 24 degrees of freedom, and a reduced variant has 21

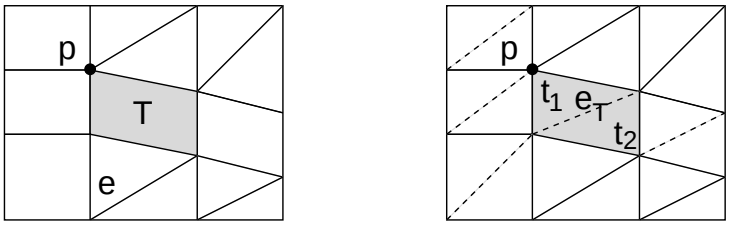

FIGURE 3.1. *Triangulation $\mathcal{T}_h$ (left) and triangulation $\mathcal{T}_h^s$ (right)*

degrees of freedom. In the following, we use the 24 dimensional space

$$S_T := \{\boldsymbol{\tau}_h \in [P_3(T)]^{2\times 2} | \quad (\tau_h)_{12} = (\tau_h)_{21}, \mathrm{div}\boldsymbol{\tau}_h \in [P_1(T)]^2\}$$

as local space on a triangle and define the global $H^{\mathrm{S}}(\mathrm{div};\Omega)$-conforming finite element space on $\mathcal{T}_h^{\mathrm{s}}$ for the stress approximation by

$$S_h^{\mathrm{s}} := \{\boldsymbol{\tau}_h \in H^{\mathrm{S}}(\mathrm{div};\Omega) | \quad \boldsymbol{\tau}_{h|_T} \in S_T, T \in \mathcal{T}_h^{\mathrm{s}}\}. \tag{3.2}$$

It can be shown [5] that the global degrees of freedom given by

- the nodal values at the vertices $p \in \mathcal{P}_h^{\mathrm{s}}$,
- the zero order moment of $\boldsymbol{\tau}_h \boldsymbol{n}_e$ in direction x_i, $i \in \{1,2\}$, on the edges $e \in \mathcal{E}_h^{\mathrm{s}}$,
- the first order moment of $\boldsymbol{\tau}_h \boldsymbol{n}_e$ in direction x_i, $i \in \{1,2\}$, on the edges $e \in \mathcal{E}_h^{\mathrm{s}}$,
- the mean values on the elements $T \in \mathcal{T}_h^{\mathrm{s}}$

yield a conforming approximation, and moreover the pairing $(S_h^{\mathrm{s}}, W_h^{\mathrm{s}})$, $W_h^{\mathrm{s}} := \{\boldsymbol{w}_h \in [L^2(\Omega)]^2 \,|\, \boldsymbol{w}_{h|_T} \in [P_1(T)]^2, T \in \mathcal{T}_h^{\mathrm{s}}\}$, satisfies a uniform inf-sup condition [5]. Thus, we have four degrees of freedom per edge, three per vertex and three per element. Originally the degrees of freedom associated with the interior of the elements are given in terms of point values at the center of gravity and not by a mean value. However it is easy to see that the uniquesolvability is still guaranteed if we replace the point value by a mean value.

Because our finite element solution $\boldsymbol{u}_h$ is defined with respect to the mesh $\mathcal{T}_h$, it is not convenient to use the space S_h^{s} being defined with respect to the mesh $\mathcal{T}_h^{\mathrm{s}}$ for the stress approximation. For $T \in \mathcal{T}_h \setminus \mathcal{T}_h^{\mathrm{s}}$, we set

$$S_T^{\mathrm{q}} := \{\boldsymbol{\tau}_h \in S_h^{\mathrm{s}}|_T \,|\, \mathrm{div}\boldsymbol{\tau}_h \in [P_1(T)]^2, \int_{e_T} (s - s_m)(\boldsymbol{\tau}_h \boldsymbol{n}_{e_T}) \cdot \boldsymbol{t}_{e_T}\, ds = 0\},$$

where s_m denotes the midpoint of the edge e_T, and $\boldsymbol{t}_{e_T}$ stands for the tangential vector on the cutting edge e_T. In terms of this local space, we define the global space $S_h \subset S_h^{\mathrm{s}}$.

$$S_h := \{\boldsymbol{\tau}_h \in S_h^{\mathrm{s}} \,|\, \boldsymbol{\tau}_h|_T \in S_T^{\mathrm{q}}, T \in \mathcal{T}_h \setminus \mathcal{T}_h^{\mathrm{s}}\}.$$

LEMMA 3.1. *Each element in S_h is uniquely defined by its*

- *nodal values at the vertices $p \in \mathcal{P}_h$,*
- *zero order moment of $\boldsymbol{\tau}_h \boldsymbol{n}_e$ in direction x_i, $i \in \{1,2\}$, on the edges $e \in \mathcal{E}_h$,*
- *first order moment of $\boldsymbol{\tau}_h \boldsymbol{n}_e$ in direction x_i, $i \in \{1,2\}$, on the edges $e \in \mathcal{E}_h$,*
- *mean values on the elements $T \in \mathcal{T}_h$.*

Proof. The proof follows the lines given in [5] for simplicial elements. Here, we have to consider the situation of decomposed quadrilaterals in more detail. Counting the number of constraints, it is sufficient to show that if $\boldsymbol{\tau}_h \in S_h$ satisfies $\boldsymbol{\tau}_h(p) = \boldsymbol{0}$, $p \in \mathcal{P}_h$, $\int_e (\boldsymbol{\tau}_h \boldsymbol{n}_e) \cdot \boldsymbol{q}_1\, ds = 0$, $\boldsymbol{q}_1 \in [P_1(e)]^2$, $e \in \mathcal{E}_h$ and $\int_T \boldsymbol{\tau}_h\, dx = \boldsymbol{0}$, $T \in \mathcal{T}_h$, then $\boldsymbol{\tau}_h = \boldsymbol{0}$. By definition of S_h, $\mathrm{div}\boldsymbol{\tau}_h|_T \in [P_1(T)]^2$, and we find

$$\int_T \mathrm{div}\boldsymbol{\tau}_h \cdot \mathrm{div}\boldsymbol{\tau}_h\, dx = -\int_T \boldsymbol{\tau}_h : \nabla \mathrm{div}\boldsymbol{\tau}_h\, dx + \int_{\partial T} (\boldsymbol{\tau}_h \boldsymbol{n}_T) \cdot \mathrm{div}\boldsymbol{\tau}_h\, ds = 0.$$

Let $t \subset T$ be an element in $\mathcal{T}_h^{\mathrm{s}}$, then Green's formula yields for $\boldsymbol{v} \in [P_0(t)]^2$

$$0 = \int_{\partial t} (\boldsymbol{\tau}_h \boldsymbol{n}_t) \cdot \boldsymbol{v} \; ds = \pm \int_{e_T} (\boldsymbol{\tau}_h \boldsymbol{n}_{e_T}) \cdot \boldsymbol{v} \; ds.$$

Setting $\boldsymbol{v} = (x_2 - x_2^m, x_1^m - x_1)^\top$, where (x_1^m, x_2^m) denotes the midpoint of the edge e_T and observing that $\boldsymbol{\epsilon}(\boldsymbol{v}) = \boldsymbol{0}$, we get

$$\boldsymbol{0} = \int_{e_T} (\boldsymbol{\tau}_h \boldsymbol{n}_{e_T}) \cdot \boldsymbol{v} \; ds = \pm \int_{e_T} (s - s_m)(\boldsymbol{\tau}_h \boldsymbol{n}_{e_T}) \cdot \boldsymbol{n}_{e_T} \; ds.$$

The definition of S_h and the previous results guarantee that the zero and first order momentums of $\boldsymbol{\tau}_h \boldsymbol{n}_e$ are zero on all edges $e \in \mathcal{E}_h^{\mathrm{s}}$. Moreover using $\mathrm{div}\boldsymbol{\tau}_h = 0$, we find

$$\int_t \boldsymbol{\tau}_h : \nabla \boldsymbol{v} = \boldsymbol{0}, \quad \boldsymbol{v} \in [P_1(t)]^2,$$

and thus all degrees of freedom of $\boldsymbol{\tau}_h$ as an element in S_h^{s} are zero. □

Now we proceed in two steps. In a first step, we define an approximation $\boldsymbol{\tau}_h \in S_h$ satisfying $\mathrm{div}\boldsymbol{\tau}_h = -\Pi_1 \boldsymbol{f}$, where Π_1 is the L^2-projection on $W_h := \{\boldsymbol{w}_h \in [L^2(\Omega)]^2 | \, \boldsymbol{w}_{h|_T} \in [P_1(T)]^2, T \in \mathcal{T}_h\}$. For this approximation, we show that in terms of $\boldsymbol{\tau}_h + \boldsymbol{\tau}^0$, where $\boldsymbol{\tau}^0 \in H^{0;\mathrm{S}}(\mathrm{div};\Omega) := \{\boldsymbol{e} \in H^{\mathrm{S}}(\mathrm{div};\Omega) | \, \mathrm{div}\boldsymbol{e} = \boldsymbol{0}\}$, we obtain an upper bound of the discretization error. To obtain a lower bound, we have to fix a suitable divergence free stress $\boldsymbol{\tau}^0$. The choice of which is motivated by being locally computable and being close to the discrete stress approximation $\boldsymbol{\sigma}_h$.

Let $\boldsymbol{\tau}_h \in S_h$ satisfy

- $\boldsymbol{\tau}_h(p) = \boldsymbol{0}$, $p \in \mathcal{P}_h$,
- $\int_e (\boldsymbol{\tau}_h \boldsymbol{n}_e) \cdot \boldsymbol{q}_1 \, ds = \int_e \boldsymbol{g}_e \cdot \boldsymbol{q}_1 \, ds$, $\boldsymbol{q}_1 \in [P_1(e)]^2$, $e \in \mathcal{E}_h$,
- $\int_T \boldsymbol{\tau}_h : \nabla \boldsymbol{v} \, dx = a_T(\boldsymbol{u}_h, \boldsymbol{v})$, $\boldsymbol{v} \in [P_1(T)]^2$, $T \in \mathcal{T}_h$.

We note that although $\dim [P_1(T)]^2 = 6$, the last condition only yields three independent equations on each element, since rigid body motions do not contribute (in other words, they yield $0 = 0$).

LEMMA 3.2. *div*$\boldsymbol{\tau}_h = -\Pi_1 \boldsymbol{f}$

Proof. By definition of S_h, we find that $\mathrm{div}\boldsymbol{\tau}_h \in W_h$, and Green's formula yields for all $\boldsymbol{v}_1 \in [P_1(T)]^2$

$$\begin{aligned} \int_T \mathrm{div}\boldsymbol{\tau}_h \cdot \boldsymbol{v}_1 \, dx &= -\int_T \boldsymbol{\tau}_h : \nabla \boldsymbol{v}_1 \, dx + \int_{\partial T} (\boldsymbol{\tau}_h \boldsymbol{n}_T) \cdot \boldsymbol{v}_1 \, ds \\ &= -a_T(\boldsymbol{u}_h, \boldsymbol{v}_1) + \int_{\partial T} \boldsymbol{g}_T \boldsymbol{v}_1 \, ds = -(\boldsymbol{f}, \boldsymbol{v}_1)_{0;T}. \end{aligned}$$

□

Now, we consider elementwise the difference between the discrete stress approximation $\boldsymbol{\sigma}_h$ and $\boldsymbol{\tau}_h + \boldsymbol{\tau}^0$, and we define

$$\eta(\boldsymbol{\tau}^0)^2 := \sum_{T \in \mathcal{T}_h} \| \mathcal{C}^{-\frac{1}{2}} (\boldsymbol{\tau}_h + \boldsymbol{\tau}^0 - \boldsymbol{\sigma}_h) \|_{0;T}^2.$$

Starting from (2.1), a straightforward computation shows that $\mathcal{C}^{-\frac{1}{2}} \boldsymbol{e}$ is given by

$$\mathcal{C}^{-\frac{1}{2}} \boldsymbol{e} = \frac{1}{\sqrt{2\mu}} \left(\boldsymbol{e} - \frac{1}{2} \left(1 - \sqrt{\frac{\mu}{\mu + \lambda}} \right) \mathrm{tr}\, \boldsymbol{e} \boldsymbol{1} \right).$$

In most a posteriori error estimates higher order terms depending on the data occur. Here, we have to take into account

$$\mathrm{osc}_1(\boldsymbol{f})^2 := \sum_{T \in \mathcal{T}_h} |T| \, \| \boldsymbol{f} - \Pi_1 \boldsymbol{f} \|_{0;T}^2,$$

where $|T|$ denotes the area of the element T. We note that if $\boldsymbol{f}$ is smooth, then $\mathrm{osc}_1(\boldsymbol{f})$ is of order h^3, whereas the discretization error in the energy norm is of $\mathcal{O}(h)$.

THEOREM 3.3. *For all $\boldsymbol{\tau}^0 \in H^{0;S}(div;\Omega)$, we obtain an upper bound for the energy norm of the discretization error in terms of $\eta(\boldsymbol{\tau}^0)$ and a higher order data oscillation term. Namely there exists a constant $C < \infty$ independent of the meshsize such that*

$$|||\boldsymbol{u} - \boldsymbol{u}_h||| \leq \eta(\boldsymbol{\tau}^0) + Cosc_1(\boldsymbol{f}).$$

Proof. We start with the definition of the energy norm, take into account the symmetry of the stress approximations and use $[\boldsymbol{\tau}_h + \boldsymbol{\tau}^0]\boldsymbol{n}_e = \mathbf{0}$ across the edges of the triangulation.

$$\begin{aligned}
|||\boldsymbol{u} - \boldsymbol{u}_h|||^2 &= \int_\Omega (\boldsymbol{\sigma} - \boldsymbol{\sigma}_h) : \boldsymbol{\epsilon}(\boldsymbol{u} - \boldsymbol{u}_h)\, dx = \int_\Omega (\boldsymbol{\sigma} - \boldsymbol{\sigma}_h) : \nabla(\boldsymbol{u} - \boldsymbol{u}_h)\, dx \\
&= \int_\Omega (\boldsymbol{\tau}_h + \boldsymbol{\tau}^0 - \boldsymbol{\sigma}_h) : \nabla(\boldsymbol{u} - \boldsymbol{u}_h)\, dx - \int_\Omega \operatorname{div}(\boldsymbol{\sigma} - \boldsymbol{\tau}_h)(\boldsymbol{u} - \boldsymbol{u}_h)\, dx \\
&= \int_\Omega \mathcal{C}^{-\frac{1}{2}}(\boldsymbol{\tau}_h + \boldsymbol{\tau}^0 - \boldsymbol{\sigma}_h) : \mathcal{C}^{\frac{1}{2}}\boldsymbol{\epsilon}(\boldsymbol{u} - \boldsymbol{u}_h)\, dx + \int_\Omega (\boldsymbol{f} - \Pi_1 \boldsymbol{f})(\boldsymbol{u} - \boldsymbol{u}_h)\, dx \\
&\leq \eta(\boldsymbol{\tau}^0)|||\boldsymbol{u} - \boldsymbol{u}_h||| + C\mathrm{osc}_1(\boldsymbol{f})|\boldsymbol{u} - \boldsymbol{u}_h|_1 \\
&\leq (\eta(\boldsymbol{\tau}^0) + C\mathrm{osc}_1(\boldsymbol{f}))|||\boldsymbol{u} - \boldsymbol{u}_h|||.
\end{aligned}$$

In the last step, we have used Korn's inequality and the boundedness of $\mathcal{C}^{-\frac{1}{2}}$. Thus the constant C in the theorem only depends on the shape regularity of the triangulation, the Lamé parameter μ and the geometry. □

REMARK 3.4. *We note that the constant C in Theorem 3.3 does not degenerate in the incompressible limit. More precisely, the operator $\mathcal{C}^{-1/2}$ can be bounded in terms of μ, and this bound does not depend on $\lambda/\mu \gg 1$.*

3.2. Lower bounds in terms of Argyris elements. Although $\eta(\boldsymbol{\tau}^0)$ provides for all $\boldsymbol{\tau}^0 \in H^{0;\mathrm{S}}(\mathrm{div};\Omega)$ an upper bound for the discretization error, we cannot expect to obtain a lower bound for arbitrary $\boldsymbol{\tau}^0$. In principle, one could solve a global minimization problem for $\boldsymbol{\tau}^0$, i.e., find $\boldsymbol{\tau}^0 \in H^{0;\mathrm{S}}(\mathrm{div};\Omega)$ such that

$$\int_\Omega \mathcal{C}^{-1}\boldsymbol{\tau}^0 : \boldsymbol{e}^0\ dx = \int_\Omega (\boldsymbol{\epsilon}(\boldsymbol{u}_h) - \mathcal{C}^{-1}\boldsymbol{\tau}_h) : \boldsymbol{e}^0\ dx, \quad \boldsymbol{e}^0 \in H^{0;\mathrm{S}}(\mathrm{div};\Omega).$$

In general this is not reasonable, and thus we carry out two simplifications. Firstly, we replace $H^{0;\mathrm{S}}(\mathrm{div};\Omega)$ by a suitable discrete approximation, and secondly we use a discrete norm equivalence to decouple the global minimization problem in local ones. We define by $S_h^{0;\mathrm{s}} := \{\boldsymbol{e}_h \in S_h^{\mathrm{s}} |\ \mathrm{div}\boldsymbol{e}_h = \mathbf{0}\}$ the divergence free subspace of S_h^{s}. The following result can be found in [5]. For convenience of the reader, we recall the proof.

LEMMA 3.5. *Let $A_h \subset H^2(\Omega)$ be the space of Argyris elements with respect to the triangulation $\mathcal{T}_h^s$, then*

$$S_h^{0;s} = J(A_h), \quad J(v) := \begin{pmatrix} v_{x_2,x_2} & -v_{x_1,x_2} \\ -v_{x_1,x_2} & v_{x_1,x_1} \end{pmatrix}.$$

Proof. We recall that Argyris elements are C^1-functions and locally in $P_5(T)$, see, e.g., [17]. Thus, it is easy to see that $J(A_h) \subset S_h^{0;\mathrm{s}}$. Six degrees of freedom are associated with the vertices (one nodal value, two first derivatives and three second derivatives), and one degree of freedom is associated with the normal derivative at the midpoint of the edge. Moreover, there exists an orthogonal decomposition of $S_h^{\mathrm{s}} = S_h^{0;\mathrm{s}} \oplus S_h^{\perp;\mathrm{s}}$, and because of the inf-sup condition we know that the dimension of $S_h^{\perp;\mathrm{s}}$ is greater or equal to $6N_T$, where N_T is the number of elements in $\mathcal{T}_h^{\mathrm{s}}$. As a result we find that the dimension of $S_h^{0;\mathrm{s}}$ is less equal $3N_p + 4N_e - 3N_T$, where N_p and N_e are the number of vertices and edges, respectively, of $\mathcal{T}_h^{\mathrm{s}}$. The dimension A_h is given by $6N_p + N_e$, and the dimension of the kernel of the Airy operator J is three. Using $N_T + N_p - N_e = 1$, we get $6N_p + N_e - 3 = 3N_p + 4N_e - 3N_T$ and thus $S_h^{0;\mathrm{s}} = J(A_h)$. □

Although the finite elements S_T in combination with the degrees of freedom used in Lemma 3.1 are not affine equivalent, we can replace the L^2-norm by a discrete mesh dependent norm. To do so, we introduce the quantities $m_p(\cdot)$, $m_e(\cdot)$ and $m_T(\cdot)$ by

$$\begin{aligned} m_p(\boldsymbol{\tau}_h) &:= \textstyle\sum_{p\in\mathcal{P}_T} \|\boldsymbol{\tau}_h(p)\|^2, \\ m_e(\boldsymbol{\tau}_h) &:= \textstyle\sum_{e\in\mathcal{E}_T} \left(\|\int_e \boldsymbol{\tau}_h \boldsymbol{n}_e \, ds\|^2 + \|\frac{1}{h_e}\int_e \boldsymbol{\tau}_h \boldsymbol{n}_e (s-s_m)\, ds\|^2 \right), \\ m_T(\boldsymbol{\tau}_h) &:= \|\textstyle\int_T \boldsymbol{\tau}_h \, dx\|^2 \end{aligned}$$

where $\|\cdot\|$ denotes the Euclidean norm in $\mathbb{R}^2$ and $\mathbb{R}^{2\times 2}$, and $\mathcal{P}_T$ stands for the set of vertices of T, and $\mathcal{E}_T$ is the set of edges of T.

LEMMA 3.6. *Let $\boldsymbol{\tau}_h \in S_T$, $T \in \mathcal{T}_h \cap \mathcal{T}_h^s$ or $\boldsymbol{\tau}_h \in S_T^q$, $T \in \mathcal{T}_h \setminus \mathcal{T}_h^s$, then there exist constants $0 < c < C < \infty$ independent on the meshsize such that*

$$c\|\boldsymbol{\tau}_h\|_{0;T}^2 \le |T| m_p(\boldsymbol{\tau}_h) + m_e(\boldsymbol{\tau}_h) + \frac{1}{|T|} m_T(\boldsymbol{\tau}_h) \le C\|\boldsymbol{\tau}_h\|_{0;T}^2, \quad T \in \mathcal{T}_h. \tag{3.3}$$

Proof. If $T \in \mathcal{T}_h$ is a triangle, we use the matrix Piola transformation

$$\boldsymbol{\tau}_h(x) = B\hat{\boldsymbol{\tau}}(\hat{x})B^\top, \tag{3.4}$$

where the affine transformation $x = B\hat{x} + b$ maps the reference element $\hat{T}$ to T. The outer normal on $\hat{T}$ is denoted by $\hat{\boldsymbol{n}}$. Since

$$\boldsymbol{n}_T = \frac{1}{\|B^{-\top}\hat{\boldsymbol{n}}\|} B^{-\top}\hat{\boldsymbol{n}},$$

we may write

$$\boldsymbol{\tau}_h \boldsymbol{n}_T = \frac{1}{\|B^{-\top}\hat{\boldsymbol{n}}\|} B\hat{\boldsymbol{\tau}}\hat{\boldsymbol{n}}. \tag{3.5}$$

Therefore the degrees of freedom on the edges are not preserved, but are transformed via the matrix B.

Now using Lemma 3.1 of [5] on the reference triangle $\hat{T}$ and the fact that all norms are equivalent in a finite-dimensional space, we get

$$\|\hat{\boldsymbol{\tau}}\|_{0;\hat{T}}^2 \sim m_p(\hat{\boldsymbol{\tau}}) + m_e(\hat{\boldsymbol{\tau}}) + m_{\hat{T}}(\hat{\boldsymbol{\tau}}), \tag{3.6}$$

where the constants of equivalence depend only on $\hat{T}$. This equivalence and the equivalences $\|B\| \sim h_T$, $\|B^{-1}\| \sim h_T^{-1}$ yield

$$\begin{aligned} \|\hat{\boldsymbol{\tau}}\|_{0;\hat{T}}^2 \sim h_T^{-4} \sum_{\hat{e}\in\mathcal{E}_{\hat{T}}} \left(\|\int_{\hat{e}} \frac{B\hat{\boldsymbol{\tau}}\hat{\boldsymbol{n}}}{\|B^{-\top}\hat{\boldsymbol{n}}\|} d\hat{s}\|^2 + \int_{\hat{e}} \frac{B\hat{\boldsymbol{\tau}}\hat{\boldsymbol{n}}}{\|B^{-\top}\hat{\boldsymbol{n}}\|} (\hat{s}-\hat{s}_m) d\hat{s}\|^2 \right) \\ + m_p(\hat{\boldsymbol{\tau}}) + m_{\hat{T}}(\hat{\boldsymbol{\tau}}). \end{aligned} \tag{3.7}$$

A scaling argument and again the above equivalences yield

$$\|\boldsymbol{\tau}_h\|_{0;T} \sim h_T^3 \|\hat{\boldsymbol{\tau}}\|_{0;\hat{T}}, \quad \|\int_T \boldsymbol{\tau}_h \, dx\| \sim h_T^4 \|\int_{\hat{T}} \hat{\boldsymbol{\tau}} \, d\hat{x}\|.$$

Using the equivalences and (3.5) in (3.7), we find the norm equivalence (3.3) for a triangular element T.

If T is a quadrilateral, we still use the matrix Piola transformation (3.4), with the affine transformation $x = B\hat{x} + b$ which maps the reference quadrilateral $\hat{T}$ to T. Here we assume that $e_{\hat{T}}$ is mapped onto e_T and that $e_{\hat{T}}$ has the endpoints $(-1,-1)$ and $(1,1)$. We note that the midpoint of $e_{\hat{T}}$ is given by $(0,0)$. On one hand we remark that (see [5, p.411])

$$\mathrm{div}\boldsymbol{\tau}_h = B\mathrm{div}\hat{\boldsymbol{\tau}}.$$

Therefore for $\boldsymbol{\tau}_h$ in S_T^{q} the property $\mathrm{div}\boldsymbol{\tau}_h \in [P_1(T)]^2$ is preserved. On the other hand the property

$$\int_{e_T} (s - s_m)(\boldsymbol{\tau}_h \boldsymbol{n}_{e_T}) \cdot \boldsymbol{t}_{e_T} \, ds = 0$$

is not preserved since

$$(\boldsymbol{\tau}_h \boldsymbol{n}_T) \cdot \boldsymbol{t}_T = \frac{1}{\|B^{-\top}\hat{\boldsymbol{n}}\| \|B\hat{\boldsymbol{t}}\|} (\hat{\boldsymbol{\tau}}\hat{\boldsymbol{n}}) \cdot B^\top B\hat{\boldsymbol{t}}. \tag{3.8}$$

Therefore we introduce the new space

$$\tilde{S}_h := \{\boldsymbol{\tau} \in S_h^{\mathrm{s}} | \quad \mathrm{div}\boldsymbol{\tau} \in [P_1(T)]^2, T \in \mathcal{T}_h\}.$$

By Lemma 3.1 and the finite-dimensionality, for $\boldsymbol{\tau}_h \in \tilde{S}_h$ and $\hat{\boldsymbol{\tau}} := B^{-1}\boldsymbol{\tau}_h B^{-\top}$ we can conclude that

$$\|\hat{\boldsymbol{\tau}}\|^2_{0;\hat{T}} \sim m_p(\hat{\boldsymbol{\tau}}) + m_e(\hat{\boldsymbol{\tau}}) + m_{\hat{T}}(\hat{\boldsymbol{\tau}}) + \left| \int_{e_{\hat{T}}} \hat{s}(\hat{\boldsymbol{\tau}}\hat{\boldsymbol{n}}) \cdot \hat{\boldsymbol{t}} d\hat{s} \right|^2, \tag{3.9}$$

where the constants in the equivalence depend only on $\hat{T}$ but not on T.

The main point is to replace the last term by

$$\left| \int_{e_{\hat{T}}} \hat{s}(\hat{\boldsymbol{\tau}}\hat{\boldsymbol{n}}) \cdot B^\top B\hat{\boldsymbol{t}} d\hat{s} \right|^2.$$

To start with, we rewrite $B^\top B\hat{\boldsymbol{t}}$ as a linear combination of $\hat{\boldsymbol{t}}$ and $\hat{\boldsymbol{n}}$

$$B^\top B\hat{\boldsymbol{t}} = \alpha_1 \hat{\boldsymbol{t}} + \alpha_2 \hat{\boldsymbol{n}},$$

where

$$\alpha_1 = B^\top B\hat{\boldsymbol{t}} \cdot \hat{\boldsymbol{t}} = \|B\hat{\boldsymbol{t}}\|^2 \sim h_T^2, \quad \alpha_2 = B^\top B\hat{\boldsymbol{t}} \cdot \hat{\boldsymbol{n}},$$

and therefore $|\alpha_2| \lesssim h_T^2$. The above identity is equivalent to

$$\hat{\boldsymbol{t}} = \frac{1}{\alpha_1} B^\top B\hat{\boldsymbol{t}} - \frac{\alpha_2}{\alpha_1}\hat{\boldsymbol{n}},$$

and thus, we have

$$\begin{aligned} \left| \int_{e_{\hat{T}}} \hat{s}(\hat{\boldsymbol{\tau}}\hat{\boldsymbol{n}}) \cdot \hat{\boldsymbol{t}} d\hat{s} \right| \lesssim h_T^{-2} \left| \int_{e_{\hat{T}}} \hat{s}(\hat{\boldsymbol{\tau}}\hat{\boldsymbol{n}}) \cdot B^\top B\hat{\boldsymbol{t}} d\hat{s} \right| \\ + \left| \int_{\hat{e}_T} \hat{s}(\hat{\boldsymbol{\tau}}\hat{\boldsymbol{n}}) \cdot \hat{\boldsymbol{n}} d\hat{s} \right|. \end{aligned} \tag{3.10}$$

To estimate this last term, we use an argument already used in Lemma 3.1, namely we take $\hat{\boldsymbol{v}} := (\hat{x}_2, -\hat{x}_1)^\top$ and use Green's formula as well as the property $\boldsymbol{\epsilon}(\hat{\boldsymbol{v}}) = \mathbf{0}$ to obtain

$$\int_{e_{\hat{T}}} \hat{s}(\hat{\boldsymbol{\tau}}\hat{\boldsymbol{n}}) \cdot \hat{\boldsymbol{n}} d\hat{s} = -\int_{\partial\hat{t}\setminus e_{\hat{T}}} (\hat{\boldsymbol{\tau}}\hat{\boldsymbol{n}}) \cdot \hat{\boldsymbol{v}} d\hat{s} + \int_{\hat{t}} \mathrm{div}\hat{\boldsymbol{\tau}} \cdot \hat{\boldsymbol{v}} d\hat{x}, \tag{3.11}$$

where $\hat{t}$ is the subtriangle of $\hat{T}$ with vertices $(-1,-1), (-1,1), (1,1)$. Since $\hat{\boldsymbol{v}}$ belongs to $[P_1(\hat{T})]^2$ and $\partial\hat{t} \setminus e_{\hat{T}} \subset \partial\hat{T}$, we deduce that

$$\left| \int_{\partial\hat{t}\setminus e_{\hat{T}}} (\hat{\boldsymbol{\tau}}\hat{\boldsymbol{n}}) \cdot \hat{\boldsymbol{v}} d\hat{s} \right|^2 \lesssim m_e(\hat{\boldsymbol{\tau}}). \tag{3.12}$$

It then remains to estimate the second term of the right-hand side of (3.11). For this purpose, writing

$$\mathrm{div}\hat{\boldsymbol{\tau}} = \begin{pmatrix} \alpha_1\hat{x}_1 + \alpha_2\hat{x}_2 + \alpha_0 \\ \beta_1\hat{x}_1 + \beta_2\hat{x}_2 + \beta_0 \end{pmatrix},$$

with some real numbers $\alpha_i, \beta_i, i = 0, 1, 2$, we see that

$$\int_{\hat{t}} \mathrm{div}\hat{\boldsymbol{\tau}} \cdot \hat{\boldsymbol{v}} d\hat{x} = \int_{\hat{t}} ((\alpha_1 - \beta_2)\hat{x}_1\hat{x}_2 + \alpha_2\hat{x}_2^2 - \beta_1\hat{x}_1^2 + \alpha_0\hat{x}_2 - \beta_0\hat{x}_1) d\hat{x}.$$

Since one readily checks that

$$0 = \int_{\hat{T}} \hat{x}_1\hat{x}_2 d\hat{x} = 2\int_{\hat{t}} \hat{x}_1\hat{x}_2 d\hat{x}, \int_{\hat{T}} \hat{x}^2 = 2\int_{\hat{t}} \hat{x}_1^2 d\hat{x}, \int_{\hat{T}} \hat{y}^2 = 2\int_{\hat{t}} \hat{x}_2^2 d\hat{x},$$

the above identity becomes

$$\int_{\hat{t}} \mathrm{div}\hat{\boldsymbol{\tau}} \cdot \hat{\boldsymbol{v}} d\hat{x} = \frac{1}{2}\int_{\hat{T}} \mathrm{div}\hat{\boldsymbol{\tau}} \cdot \hat{\boldsymbol{v}} d\hat{x} + \int_{\hat{t}} (\alpha_0\hat{x}_2 - \beta_0\hat{x}_1) d\hat{x}.$$

Applying Green's formula on $\hat{T}$, we obtain

$$\int_{\hat{t}} \mathrm{div}\hat{\boldsymbol{\tau}} \cdot \hat{\boldsymbol{v}} d\hat{x} = \frac{1}{2}\int_{\partial\hat{T}} (\hat{\boldsymbol{\tau}}\hat{\boldsymbol{n}}) \cdot \hat{\boldsymbol{v}} d\hat{s} + \int_{\hat{t}} (\alpha_0\hat{x}_2 - \beta_0\hat{x}_1) d\hat{s}.$$

On the other hand, one may remark that

$$4(\alpha_0, \beta_0)^\top = \int_{\hat{T}} \mathrm{div}\hat{\boldsymbol{\tau}} d\hat{x} = \int_{\partial\hat{T}} \hat{\boldsymbol{\tau}} \cdot \hat{\boldsymbol{n}} d\hat{s}.$$

These two identities imply that

$$\left| \int_{\hat{t}} \mathrm{div}\hat{\boldsymbol{\tau}} \cdot \hat{\boldsymbol{v}} d\hat{x} \right|^2 \lesssim m_e(\hat{\boldsymbol{\tau}}). \tag{3.13}$$

The upper bounds (3.12) and (3.13) in combination with the identity (3.11) yield

$$\left| \int_{e_{\hat{T}}} \hat{s}(\hat{\boldsymbol{\tau}}\hat{\boldsymbol{n}}) \cdot \hat{\boldsymbol{n}} d\hat{s} \right|^2 \lesssim m_e(\hat{\boldsymbol{\tau}}).$$

This estimate used in (3.10) leads to

$$\left| \int_{e_{\hat{T}}} \hat{s}(\hat{\boldsymbol{\tau}}\hat{\boldsymbol{n}}) \cdot \hat{\boldsymbol{t}} d\hat{s} \right|^2 \lesssim h_T^{-4} \left| \int_{e_{\hat{T}}} \hat{s}(\hat{\boldsymbol{\tau}}\hat{\boldsymbol{n}}) \cdot B^\top B\hat{\boldsymbol{t}} d\hat{s} \right|^2 + m_e(\hat{\boldsymbol{\tau}}).$$

Inserting this estimate in (3.9) allows us to conclude with

$$\|\hat{\boldsymbol{\tau}}\|_{0;\hat{T}}^2 \lesssim m_p(\hat{\boldsymbol{\tau}}) + m_e(\hat{\boldsymbol{\tau}}) + m_{\hat{T}}(\hat{\boldsymbol{\tau}}) + \frac{1}{h_T^4} \left| \int_{\hat{e}_T} \hat{s}(\hat{\boldsymbol{\tau}}\hat{\boldsymbol{n}}) \cdot B^\top B\hat{\boldsymbol{t}} d\hat{s} \right|^2. \tag{3.14}$$

Similarly we can prove that for $\hat{\boldsymbol{\tau}} := B^{-1}\boldsymbol{\tau}_h B^{-}$ that

$$m_p(\hat{\boldsymbol{\tau}}) + m_e(\hat{\boldsymbol{\tau}}) + m_{\hat{T}}(\hat{\boldsymbol{\tau}}) + \frac{1}{h_T^4} \left| \int_{e_{\hat{T}}} \hat{s}(\hat{\boldsymbol{\tau}}\hat{\boldsymbol{n}}) \cdot B^\top B\hat{\boldsymbol{t}} d\hat{s} \right|^2 \lesssim \|\hat{\boldsymbol{\tau}}\|_{0;\hat{T}}^2. \tag{3.15}$$

Let $\boldsymbol{\tau}_h \in S_h \subset \tilde{S}_h$ and $T \in \mathcal{T}_h \setminus \mathcal{T}_h^{\mathrm{s}}$, then the definition of S_h, (3.4) and (3.8) yield

$$\int_{e_{\hat{T}}} \hat{s}(\hat{\boldsymbol{\tau}}\hat{\boldsymbol{n}}) \cdot B^\top B\hat{\boldsymbol{t}} d\hat{s} = 0.$$

Therefore the integral term on $e_{\hat{T}}$ in (3.14) and in (3.15) disappears and, as for triangular elements, going back to T, we get the norm equivalence.

□

This lemma motivates our choice for the definition of $\boldsymbol{\tau}^0$. Let us denote by ϕ_p^{ij}, $p \in \mathcal{P}_h$, $1 \le i \le j \le 2$, the nodal Argyris basis functions associated with the vertex p and the second derivative with respect to the coordinates x_i and x_j, the nodal Argyris basis functions associated with the edge is denoted by ϕ_e, $e \in \mathcal{E}_h^{\mathrm{s}}$. This one is rescaled such that $\int_e (\partial\phi_e)/(\partial \boldsymbol{n}_e)\, ds = h_e$. We denote the subset of A_h spanned by these basis functions by A_h^0, i.e., $A_h^0 := \mathrm{span}\{\phi_p^{ij}, p \in \mathcal{P}_h, 1 \le i \le j \le 2, \phi_e, e \in \mathcal{E}_h^{\mathrm{s}}\}$.

LEMMA 3.7. *Let $\phi \in A_h^0$, then*

$$\int_e J(\phi)\boldsymbol{n}_e \, ds = \mathbf{0}, \quad \int_e (s - s_m)(J(\phi)\boldsymbol{n}_e) \cdot \boldsymbol{n}_e \, ds = 0, \quad e \in \mathcal{E}_h^s.$$

Let $\phi = \sum_{p\in\mathcal{P}_h} \sum_{1\le i\le j\le 2} \alpha_p^{ij}\phi_p^{ij} + \sum_{e\in\mathcal{E}_h^s} \beta_e\phi_e$, then

$$\int_e (s - s_m)(J(\phi)\boldsymbol{n}_e) \cdot \boldsymbol{t}_e \, ds = \beta_e h_e, \quad e \in \mathcal{E}_h^s.$$

Proof. A straightforward computation shows

$$J(\phi)\boldsymbol{n}_e = \begin{pmatrix} \phi_{2,\boldsymbol{t}_e} \\ -\phi_{1,\boldsymbol{t}_e} \end{pmatrix}, \quad (J(\phi)\boldsymbol{n}_e) \cdot \boldsymbol{n}_e = \phi_{\boldsymbol{t}_e,\boldsymbol{t}_e},$$

where $\phi_{i,\boldsymbol{t}_e}$ has to be understood as derivative of ϕ in x_i and $\boldsymbol{t}_e$ direction and $\phi_{\boldsymbol{t}_e,\boldsymbol{t}_e}$ as second derivative in $\boldsymbol{t}_e$ direction. From this and the fact that ϕ and all its first order derivatives are zero at all vertices, the first part of the assertion follows by integration. Now, we consider the tangential component of $J(\phi)\boldsymbol{n}_e$, and find

$$(J(\phi)\boldsymbol{n}_e) \cdot \boldsymbol{t}_e = -\phi_{\boldsymbol{n}_e,\boldsymbol{t}_e}.$$

Then integration by parts yields

$$\int_e (s - s_m)(J(\phi)\boldsymbol{n}_e) \cdot \boldsymbol{t}_e \, ds = \int_e \phi_{\boldsymbol{n}_e} \, ds = \beta_e h_e.$$

□

Now, we define our divergence free contribution $\boldsymbol{\tau}^0 := J(\psi)$, where ψ is a linear combination of these Argyris basis functions. We note that we do not use all Argyris functions and that other choices are possible. Let $Q : V_h \longrightarrow [V_h^{\mathrm{s}}]^{2\times 2;\mathrm{S}}$, where $[V_h^{\mathrm{s}}]^{2\times 2;\mathrm{S}}$ is the space of symmetric tensors of which the components are in V_h^{s}, $V_h^{\mathrm{s}} := \{v \in H^1(\Omega),\, v_{|T} \in P_1(T), T \in \mathcal{T}_h^{\mathrm{s}}\}$, be a locally defined operator such that for all $T \in \mathcal{T}_h^{\mathrm{s}}$

$$\|Q\boldsymbol{v}_h - \mathcal{C}\boldsymbol{\epsilon}(\boldsymbol{v}_h)\|_{0;T}^2 \le C \sum_{e\in\mathcal{E}_T^{\mathrm{loc}}} h_e \|[\mathcal{C}\boldsymbol{\epsilon}(\boldsymbol{v}_h)\boldsymbol{n}_e]\|_{0;e}^2, \tag{3.16}$$

where $\mathcal{E}_T^{\mathrm{loc}}$ is a suitable set of edges being in the neighborhood of T. Such an operator can be quite easily constructed, e.g., we can set

$$Q\boldsymbol{v}_h(p) := \frac{1}{N_T^p} \sum_{T\in\mathcal{T}_p} \mathcal{C}\boldsymbol{\epsilon}(\boldsymbol{v}_h)_{|T}(p),$$

where $\mathcal{T}_p$ is the set of all elements $T \in \mathcal{T}_h^{\mathrm{s}}$ such that p is a vertex of T, and N_T^p is the number of elements in $\mathcal{T}_p$. For this choice, standard scaling arguments lead to

$$\|Q\boldsymbol{v}_h - \mathcal{C}\boldsymbol{\epsilon}(\boldsymbol{v}_h)\|_{0;T}^2 \leq C \sum_{e \in \mathcal{E}_T^{\mathrm{loc}}} h_e \|[\mathcal{C}\boldsymbol{\epsilon}(\boldsymbol{v}_h)]\|_{0;e}^2.$$

Then the tangential component of $\mathcal{C}\boldsymbol{\epsilon}(\boldsymbol{v}_h)$ can be removed in the upper bound by taking into account that $[\nabla \boldsymbol{v}_h \boldsymbol{t}_e] = \boldsymbol{0}$. More precisely, this implies that

$$[\mathcal{C}\boldsymbol{\epsilon}(\boldsymbol{v}_h)] = M[\mathcal{C}\boldsymbol{\epsilon}(\boldsymbol{v}_h)\boldsymbol{n}_e]C,$$

where M is a 2×2 matrix and C a 1×2 one. The coefficients of which depend on the Lamé parameters. We note that more sophisticated choices of Q are possible. Then weights depending on the area of the elements and on the Lamé parameters in case of discontinuities enter.

Now, we define

$$\psi := \sum_{p \in \mathcal{P}_h} \sum_{1 \leq i \leq j \leq 2} \alpha_p^{ij} \phi_p^{ij} + \sum_{e \in \mathcal{E}_h^{\mathrm{n}}} \beta_e \phi_e, \tag{3.17}$$

where the coefficients are given by $\beta_e := 1/h_e \int_e (s - s_m) \boldsymbol{\sigma}_h \boldsymbol{n}_e \cdot \boldsymbol{t}_e \; ds$ and $\alpha_p^{11} := (Q\boldsymbol{u}_h(p))_{22}$, $\alpha_p^{12} := -(Q\boldsymbol{u}_h(p))_{12}$, $\alpha_p^{22} := (Q\boldsymbol{u}_h(p))_{11}$. The discrete surface traction $\boldsymbol{\sigma}_h \boldsymbol{n}_e$ is well defined on $e \in \mathcal{E}_h^{\mathrm{n}}$. We note that if the two elements T_1, $T_2 \in \mathcal{T}_h$ sharing the edge $e \in \mathcal{E}_h$ are triangles, then $\{\boldsymbol{\sigma}_h \boldsymbol{n}_e\} \in P_0(e)$ and thus $\int_e (s - s_m)\{\boldsymbol{\sigma}_h \boldsymbol{n}_e\} \cdot \boldsymbol{t}_e \; ds = 0$. Here $\{\cdot\}$ denotes the average across the edges. This observation motivates the use of the edges $e \in \mathcal{E}_h^{\mathrm{n}}$ in the definition (3.17), but to skip the ones in $\mathcal{E}_h$.

Now, we are in the setting to define our error estimator

$$\eta^2 := \sum_{T \in \mathcal{T}_h} \eta_T^2 := \sum_{T \in \mathcal{T}_h} \|\mathcal{C}^{-\frac{1}{2}}(\boldsymbol{\tau}_h + J(\psi) - \boldsymbol{\sigma}_h)\|_{0;T}^2. \tag{3.18}$$

Because $J(\psi) \in H^{0;\mathrm{S}}(\mathrm{div}; \Omega)$, we are in the setting of Theorem 3.3 and η provides an upper bound of the discretization error. The following theorem shows that η_T provides a local lower bound.

THEOREM 3.8. *There exists a constant independent of the meshsize such that*

$$c\eta_T^2 \leq \|\mathcal{C}^{\frac{1}{2}}\boldsymbol{\epsilon}(\boldsymbol{u} - \boldsymbol{u}_h)\|_{0;\omega_T}^2 + osc_{1;\omega_T}(\boldsymbol{f}), \quad T \in \mathcal{T}_h,$$

where ω_T is the union of all elements $\tilde{T} \in \mathcal{T}_h$ such that $\partial T \cap \partial \tilde{T} \neq \emptyset$.

Proof. We start with the observation that the components of $\boldsymbol{\sigma}_h = \mathcal{C}\boldsymbol{\epsilon}(\boldsymbol{u}_h)$ restricted to $T \in \mathcal{T}_h$ are in $P_1(T)$. Moreover the definition of β_e in (3.17) and Lemma 3.7 yield that

$$\int_{e_T} (s - s_m)((J(\psi) - \boldsymbol{\sigma}_h)\boldsymbol{n}_e) \cdot \boldsymbol{t}_e \; ds = 0, \quad e_T \in \mathcal{E}_h^{\mathrm{n}},$$

and thus $J(\psi) - \boldsymbol{\sigma}_h$ is an element in S_T if $T \in \mathcal{T}_h \cap \mathcal{T}_h^{\mathrm{s}}$ and in S_T^{q} for $T \in \mathcal{T}_h \setminus \mathcal{T}_h^{\mathrm{s}}$, and we can apply Lemma 3.6 to $\boldsymbol{\tau}_h + J(\psi) - \boldsymbol{\sigma}_h$. Using Lemma 3.6, we have to estimate the quantities $m_e(\cdot)$, $m_p(\cdot)$ and $m_T(\cdot)$. In a first step, we consider $m_T(\cdot)$

$$m_T(\boldsymbol{\tau}_h + J(\psi) - \boldsymbol{\sigma}_h) = \| \int_T (\boldsymbol{\tau}_h + J(\psi) - \boldsymbol{\sigma}_h) \; dx\|^2 = \| \int_T J(\psi) \; dx\|^2,$$

since the definition of $\boldsymbol{\tau}_h$ yields $\int_T \boldsymbol{\tau}_h dx = \int_T \boldsymbol{\sigma}_h dx$. Let $\boldsymbol{v} \in RM^{\mathrm{c}}(T)$, where $RM^{\mathrm{c}}(T) := \mathrm{span}\{(x_2, x_1)^T, (x_1, 0)^T, (0, x_2)^T\}$, then we find

$$\int_T J(\psi) : \nabla \boldsymbol{v} \; dx = -\int_T \mathrm{div} J(\psi) \cdot \boldsymbol{v} \; dx + \int_{\partial T} (J(\psi)\boldsymbol{n}_T) \cdot \boldsymbol{v} \; ds = \int_{\partial T} (J(\psi)\boldsymbol{n}_T) \cdot \boldsymbol{v} \; ds.$$

In terms of Lemma 3.7 and the definition (3.17) of ψ, we find $m_T(\boldsymbol{\tau}_h + J(\psi) - \boldsymbol{\sigma}_h) = 0$.

Secondly, we consider $m_p(\cdot)$. The definition of $\boldsymbol{\tau}_h$ gives $\boldsymbol{\tau}_h(p) = \mathbf{0}$, and the assumption (3.16) on the operator Q gives

$$\begin{aligned} m_p(\boldsymbol{\tau}_h + J(\psi) - \boldsymbol{\sigma}_h) &= m_p(J(\psi) - \boldsymbol{\sigma}_h) = \textstyle\sum_{p\in\mathcal{P}_T} \|Q\boldsymbol{u}_h(p) - \mathcal{C}\boldsymbol{\epsilon}(\boldsymbol{u}_h)_{|T}(p)\|^2 \\ &\leq \tfrac{C}{|T|}\|Q\boldsymbol{u}_h - \mathcal{C}\boldsymbol{\epsilon}(\boldsymbol{u}_h)\|^2_{0;T} \leq \tfrac{C}{|T|}\textstyle\sum_{e\in\mathcal{E}_T^{\mathrm{loc}}} h_e\|[\boldsymbol{\sigma}_h\boldsymbol{n}_e]\|^2_{0;e}. \end{aligned}$$

In a third step, we focus on $m_e(\cdot)$. The definition of $\boldsymbol{\tau}_h$ allows us to replace $\boldsymbol{\tau}_h\boldsymbol{n}_e$ by $\boldsymbol{g}_e$. Moreover using Lemma 3.7 and the definition (3.17) of ψ, we find that $J(\psi)\boldsymbol{n}_e$ does not contribute to the integrals in the definition of $m_e(\cdot)$. Then the Cauchy–Schwarz inequality yields

$$m_e(\boldsymbol{\tau}_h + J(\psi) - \boldsymbol{\sigma}_h) \leq C \sum_{e\in\mathcal{E}_T} h_e\|\boldsymbol{g}_e - \boldsymbol{\sigma}_{h|T}\boldsymbol{n}_e\|^2_{0;e}.$$

By Lemma 3.6, we find the upper bound

$$\eta_T^2 \leq C \sum_{e\in\mathcal{E}_T^{\mathrm{loc}}} h_e\|\boldsymbol{g}_e - \boldsymbol{\sigma}_{h|T}\boldsymbol{n}_e\|^2_{0;e}.$$

This term is a part of the equilibrated error estimator, and we refer to [2] for an upper bound in terms of the discretization error. □

We note that the higher order terms are, in general, expressed in terms of $\|\boldsymbol{f}-\Pi_0\boldsymbol{f}\|_{0;T}$ instead of $\|\boldsymbol{f} - \Pi_1\boldsymbol{f}\|_{0;T}$. Following the lines in [29] and using element bubble functions as weights, we can replace $\|\boldsymbol{f} - \Pi_0\boldsymbol{f}\|_{0;T}$ by $\|\boldsymbol{f} - \Pi_1\boldsymbol{f}\|_{0;T}$.

REMARK 3.9. *By defining in a local postprocess a new approximation for the stress by* $\boldsymbol{\sigma}_h^{post} := \frac{1}{2}(\boldsymbol{\sigma}_h + \boldsymbol{\tau}_h + J(\psi))$*, we find that the error estimator* 0.5η *is up to higher order terms equal to the error* $\|\mathcal{C}^{-1/2}(\boldsymbol{\sigma} - \boldsymbol{\sigma}_h^{post})\|_0$*, see, e.g., [24] for the Laplace equation, and for more general concepts and basic techniques [23].*

REMARK 3.10. *We note that the constant in the higher order term for the upper bound does not degenerate in the nearly incompressible limit. In that case, the standard displacement based formulation shows volume locking and has to be replaced by a stable approach. This can be realized, e.g., by replacing the bilinear form* $a(\cdot,\cdot)$ *by a mesh dependent one. Then the upper bound also holds. This observation makes the approach quite interesting in the nearly incompressible range.*

4. Local realization of the error estimator. In this section, we provide a possibility to compute the error estimator from $\boldsymbol{g}_e$ by solving scalar equations and using basis functions on the reference element. Without loss of generality, we restrict ourselves to the case of a simplicial triangulation $\mathcal{T}_h = \mathcal{T}_h^{\mathrm{s}}$. Using the Piola transformation for tensor quantities, the nodal basis functions on the reference element can be transformed. However this does not guarantee an affine equivalent family. Here, we proceed differently and do not use a nodal basis with respect to the specified degrees of freedom, but a basis which forms a lower triangular matrix with many zero entries.

Let us denote by λ_e the nodal quadratic Lagrange finite element associated with the midpoint m_e of the edge e, i.e., $\lambda_e(m_{\tilde{e}}) = \delta_{e\tilde{e}}$. Concerning the basis functions for the Argyris element, there exists locally a second set of degrees of freedoms such that the arising nodal basis functions are affine equivalent, see, e.g., [17]. We use the symbol ϕ for the nodal Argyris basis functions associated with the original set of degrees of freedom and the symbol $\tilde{\phi}$ for the ones associated with the affine set. The main difference compared to the standard set is that the derivatives at the vertices p_j, $1 \leq j \leq 3$, are not prescribed with respect to the coordinates x_i, $1 \leq i \leq 2$, but with respect to $p_{j+1} - p_j$ and $p_{j+2} - p_j$, see Figure 4.1.

Here and in the following, the notation $j+1$ and $j+2$ has to be understood in the sense of $\mathrm{mod}_3(j+1)$ and $\mathrm{mod}_3(j+2)$, respectively, and 0 is identified with 3. The normal derivatives at the midpoints are also replaced. The degrees of freedom associated with the normal derivative at the midpoint m_{e_i} of the edges e_i is substituted by the mean value of the derivative in direction

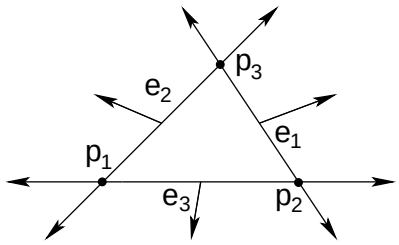

FIGURE 4.1. *Local notation on an element*

$p_i - m_{e_i}$. We specify elementwise the following set of 24 symmetric matrix valued functions:

$$\begin{aligned}
\boldsymbol{\varphi}_T^i &:= \lambda_{e_i} \boldsymbol{t}_{e_i} \boldsymbol{t}_{e_i}^\top, \quad 1 \le i \le 3, \\
\boldsymbol{\varphi}_{e_i}^{\boldsymbol{n};0} &:= \lambda_{e_i} \boldsymbol{n}_{e_i} \boldsymbol{n}_{e_i}^\top, \quad 1 \le i \le 3, \\
\boldsymbol{\varphi}_{e_i}^{\boldsymbol{t};0} &:= \lambda_{e_i} (\boldsymbol{t}_{e_i} \boldsymbol{n}_{e_i}^\top + \boldsymbol{n}_{e_i} \boldsymbol{t}_{e_i}^\top), \quad 1 \le i \le 3, \\
\boldsymbol{\varphi}_{e_i}^{\boldsymbol{n};1} &:= J(\tilde{\phi}_{p_{i+2}}^{i+1} - \tilde{\phi}_{p_{i+1}}^{i+2}), \quad 1 \le i \le 3, \\
\boldsymbol{\varphi}_{e_i}^{\boldsymbol{t};1} &:= J(\phi_{e_i}), \quad 1 \le i \le 3, \\
\boldsymbol{\varphi}_{p_i}^{k;j} &:= J(\phi_{p_i}^{kj}), \quad 1 \le i \le 3, 1 \le k \le j \le 2,
\end{aligned} \tag{4.1}$$

where e_i and p_i are the edges and vertices of the triangles, and $\tilde{\phi}_{p_i}^j$ is the nodal basis function satisfying

$$\nabla \tilde{\phi}_{p_i}^j(p_i) \cdot (p_j - p_i) = 1, \quad i \ne j,$$

whereas all other degrees of freedom are zero. Upper indices 0 and 1 stand for the zero and first order momentums and upper indices $\boldsymbol{n}$ and $\boldsymbol{t}$ stand for the normal and tangential direction, respectively. It is obvious that all given functions are in S_T (note that the nodal function $\tilde{\phi}_{p_i}^j$ is a linear combination of the standard nodal Argyris basis function). We show that these 24 functions generate any element of S_T and thus form a basis of S_T. Moreover using this set, we shall see that the matrix defining $\boldsymbol{\tau}_h + J(\psi)$ is a lower triangular matrix that is easily computable. Indeed in the rest of this section, we provide the construction which will be carried out in six steps. We set locally

$$\boldsymbol{\tau}_h^{\mathrm{g}} = \sum_{i=1}^{3} \left(a_i \boldsymbol{\varphi}_T^i + b_i \boldsymbol{\varphi}_{e_i}^{\boldsymbol{n};0} + c_i \boldsymbol{\varphi}_{e_i}^{\boldsymbol{t};0} + d_i \boldsymbol{\varphi}_{e_i}^{\boldsymbol{n};1} + \varepsilon_i \boldsymbol{\varphi}_{e_i}^{\boldsymbol{t};1} + \sum_{1 \le k \le j \le 2} f_i^{kj} \boldsymbol{\varphi}_{p_i}^{k;j}) \right).$$

To start, we consider the degrees of freedom associated with the lowest and first order momentum in normal direction. In the first step, we define the coefficients b_i by

$$b_i := \frac{\int_{e_i} \boldsymbol{g}_T \cdot \boldsymbol{n}_T ds}{\int_{e_i} (\boldsymbol{\varphi}_{e_i}^{\boldsymbol{n};0} \boldsymbol{n}_T) \cdot \boldsymbol{n}_T ds} = \frac{\int_{e_i} \boldsymbol{g}_T \cdot \boldsymbol{n}_T ds}{\int_{e_i} \lambda_{e_i} ds} = \frac{3}{2h_{e_i}} \int_{e_i} \boldsymbol{g}_T \cdot \boldsymbol{n}_T ds,$$

and observe that $(\boldsymbol{\varphi}_{e_i}^{\boldsymbol{n};0} \boldsymbol{n}_T) \cdot \boldsymbol{n}_T = (\lambda_{e_i} \boldsymbol{n}_T \boldsymbol{n}_T^\top \boldsymbol{n}_T) \cdot \boldsymbol{n}_T = \lambda_{e_i} \boldsymbol{n}_T^\top \boldsymbol{n}_T = \lambda_{e_i}$. In the second step, we set the coefficients d_i to

$$d_i := \frac{\int_{e_i} (s - s_m) \boldsymbol{g}_T \cdot \boldsymbol{n}_T ds}{\int_{e_i} (s - s_m) (\boldsymbol{\varphi}_{e_i}^{\boldsymbol{n};1} \boldsymbol{n}_T) \cdot \boldsymbol{n}_T ds} = \frac{1}{h_{e_i}} \int_{e_i} (s - s_m) \boldsymbol{g}_T \cdot \boldsymbol{n}_T ds$$

and use the definition of $\boldsymbol{\varphi}_{e_i}^{\boldsymbol{n};1}$. We note that the steps 1 and 2 are independent. Now, we define in steps 3 and 4 the coefficients associated with the moments in tangential direction. Let

$\boldsymbol{q} := \sum_{i=1}^{3} d_i \boldsymbol{\varphi}_{e_i}^{\boldsymbol{n};1}$, then we define in step 3

$$c_i := \frac{\int_{e_i} (\boldsymbol{g}_T - \boldsymbol{q}\boldsymbol{n}_T) \cdot \boldsymbol{t}_T ds}{\int_{e_i} (\boldsymbol{\varphi}_{e_i}^{\boldsymbol{t};0} \boldsymbol{n}_T) \cdot \boldsymbol{t}_T ds} = \frac{3}{2h_{e_i}} \int_{e_i} (\boldsymbol{g}_T - \boldsymbol{q}\boldsymbol{n}_T) \cdot \boldsymbol{t}_T ds.$$

Here, we have used $((\boldsymbol{t}_T \boldsymbol{n}_T^\top + \boldsymbol{n}_T \boldsymbol{t}_T^\top)\boldsymbol{n}_T) \cdot \boldsymbol{t}_T = \boldsymbol{t}_T \cdot \boldsymbol{t}_T = 1$ and the definition of $\boldsymbol{\varphi}_{e_i}^{\boldsymbol{t};0}$. Step 4 is given by

$$\varepsilon_i := \frac{\int_{e_i} (s - s_m)(\boldsymbol{g}_T - \boldsymbol{q}\boldsymbol{n}_T) \cdot \boldsymbol{t}_T ds}{\int_{e_i} (s - s_m)(\boldsymbol{\varphi}_{e_i}^{\boldsymbol{t};1} \boldsymbol{n}_T) \cdot \boldsymbol{t}_T ds} = \frac{1}{h_{e_i}} \int_{e_i} (s - s_m)(\boldsymbol{g}_T - \boldsymbol{q}\boldsymbol{n}_T) \cdot \boldsymbol{t}_T ds.$$

We note that the ordering of the steps 3 and 4 is arbitrary. Step 5 is independent of all the previous four steps. Following the definition (3.17), the coefficients f_i^{kj} are defined by

$$\begin{aligned} f_i^{11} &:= (Q\boldsymbol{u}_h(p_i))_{22}, \\ f_i^{12} &:= -(Q\boldsymbol{u}_h(p_i))_{12}, \\ f_i^{22} &:= (Q\boldsymbol{u}_h(p_i))_{11}. \end{aligned}$$

Finally in the last step, we fix the degrees of freedom associated with the interior of the element. Let $\boldsymbol{q} := \boldsymbol{\tau}_h^{\mathrm{g}} - \sum_{i=1}^{3} a_i \boldsymbol{\varphi}_T^i$, then we define

$$\begin{aligned} a_i &:= \frac{\int_T (\boldsymbol{\sigma}_h - \boldsymbol{q}) : (\boldsymbol{n}_{e_{i+1}} \boldsymbol{n}_{e_{i+2}}^\top + \boldsymbol{n}_{e_{i+2}} \boldsymbol{n}_{e_{i+1}}^\top) dx}{\int_T \boldsymbol{\varphi}_T^i : (\boldsymbol{n}_{e_{i+1}} \boldsymbol{n}_{e_{i+2}}^\top + \boldsymbol{n}_{e_{i+2}} \boldsymbol{n}_{e_{i+1}}^\top) dx} \\ &= \frac{-3h_{e_i}^2 h_{e_{i+1}} h_{e_{i+2}}}{8|T|^3} \int_T (\boldsymbol{\sigma}_h - \boldsymbol{q}) : (\boldsymbol{n}_{e_{i+1}} \boldsymbol{n}_{e_{i+2}}^\top + \boldsymbol{n}_{e_{i+2}} \boldsymbol{n}_{e_{i+1}}^\top) dx. \end{aligned}$$

Here, we have used that

$$(\boldsymbol{n}_{e_{i+1}} \boldsymbol{n}_{e_{i+2}}^\top + \boldsymbol{n}_{e_{i+2}} \boldsymbol{n}_{e_{i+1}}^\top) : \boldsymbol{t}_{e_i} \boldsymbol{t}_{e_i}^\top = 2\boldsymbol{n}_{e_{i+1}}^\top \boldsymbol{t}_{e_i} \boldsymbol{n}_{e_{i+2}}^\top \boldsymbol{t}_{e_i} = -4|T|^2/(h_{e_i}^2 h_{e_{i+1}} h_{e_{i+2}}).$$

LEMMA 4.1. *We find that* $\boldsymbol{\tau}_h^g = (\boldsymbol{\tau}_h + J(\psi))_{|_T}$.

Proof. A straightforward computation taking into account the definition (4.1) and the properties of the Argyris functions and the Airy operator shows the equality. We note that the elements $(\boldsymbol{n}_{e_{i+1}} \boldsymbol{n}_{e_{i+2}}^\top + \boldsymbol{n}_{e_{i+2}} \boldsymbol{n}_{e_{i+1}}^\top)$, $1 \le i \le 3$, form a basis of the symmetric matrices with constant coefficients. Moreover, we observe that $(\boldsymbol{n}_{e_{i+1}} \boldsymbol{n}_{e_{i+2}}^\top + \boldsymbol{n}_{e_{i+2}} \boldsymbol{n}_{e_{i+1}}^\top) : \boldsymbol{t}_{e_j} \boldsymbol{t}_{e_j}^\top = 0$ for $j \in \{i+1, i+2\}$. Due to this biorthogonality, the coefficients a_i decouple and can be computed by scalar equations. □

REMARK 4.2. *The construction of the error estimator and the proof of Theorem 3.8 shows that we can replace the definition of* ε_i *by*

$$\frac{\int_{e_i} (s - s_m)(-\boldsymbol{q}\boldsymbol{n}_T) \cdot \boldsymbol{t}_T ds}{\int_{e_i} (s - s_m)(\boldsymbol{\varphi}_{e_i}^{\boldsymbol{t};1} \boldsymbol{n}_T) \cdot \boldsymbol{t}_T ds} = \frac{1}{h_{e_i}} \int_{e_i} (s_m - s)(\boldsymbol{q}\boldsymbol{n}_T) \cdot \boldsymbol{t}_T ds.$$

and still get upper and lower bounds for the discretization error.

5. Numerical Results.

5.1. L-shaped domain. In the first example, we consider the problem

$$-\operatorname{div} \boldsymbol{\sigma} = \boldsymbol{0} \quad \text{in } \Omega$$

with Dirichlet boundary conditions computed from the exact solution, where Ω is the L-shaped domain described by the polygon $(0,0), (1,0), (1,1), (-1,1), (-1,-1), (0,-1)$. We set the Lamé–parameters $\lambda = 4.6$ and $\mu = 0.63$, the material coefficients of lead. The exact solution for this problem is

$$\boldsymbol{u}(r,\theta) = \begin{pmatrix} r^\alpha(-(1+A_\alpha)\sin(\alpha\theta) + \sin((\alpha-2)\theta)) \\ r^\alpha(-\cos(\alpha\theta) + \cos((\alpha-2)\theta)) \end{pmatrix}$$

with $A_\alpha = \frac{2(\lambda+3\mu)}{(\lambda+\mu)\alpha}$ and $\alpha = 0.5788772315$.

Figure 5.1 shows the initial and refined meshes. Here, we use a triangulation in quadrilaterals. The solution has a singularity at the re–entrant corner, so the adapted meshes are much more refined there.

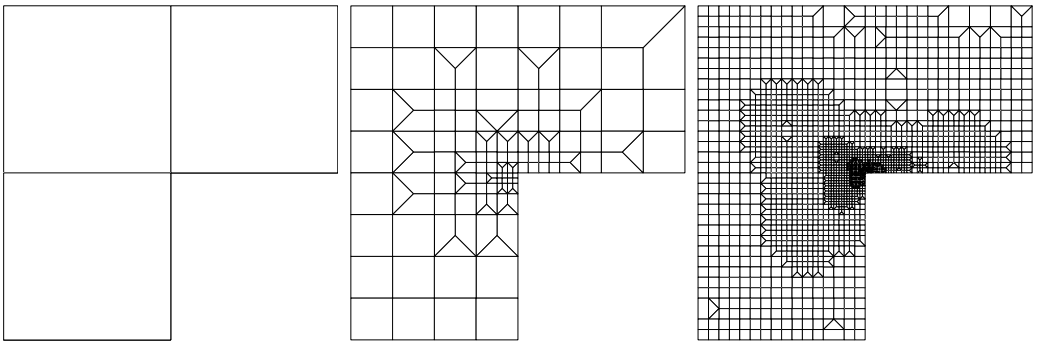

FIGURE 5.1. *Initial mesh (left) and mesh after 5 (middle) and 10 (right) refinement steps for the example of subsection 5.1*

If one computes the convergence rates s, where the square root of the quotient of the number of nodes in step i and the number of nodes in step $i+1$ to the power of s is the quotient of the error in step $i+1$ and the error in step i, the averaged value is 1.0816 for the estimated and 1.0898 for the exact error for adaptive refinement. For uniform refinement, the square root of the quotient of the number of nodes in step i and the number of nodes in step $i+1$ is approximately $1/2$, so we compute s from $(1/2)^s = \mathrm{err}_{i+1}/\mathrm{err}_i$. In that case, the convergence rates tend to α.

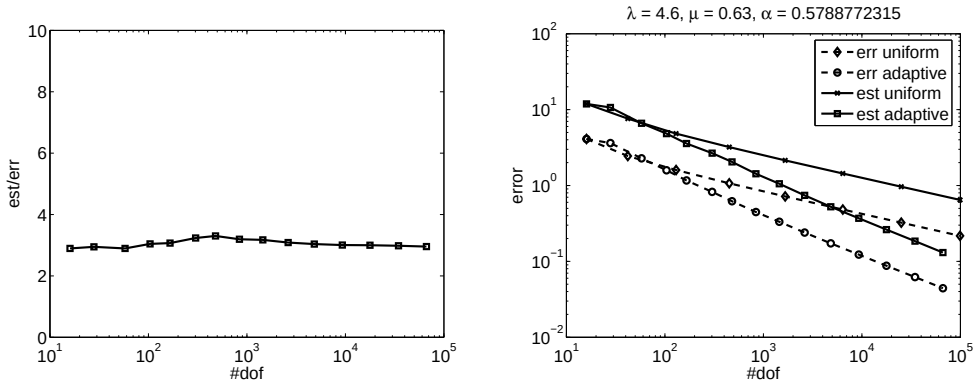

FIGURE 5.2. *Ratio between estimated and exact error (left) and error and error estimator for uniform and adaptive refinement (right) for the example of subsection 5.1*

Figure 5.2 shows on the left the ratio between estimated and exact error. Asymptotically, this ratio tends to a constant value which is a measure for the quality of the error estimator.The closer it is to one, the better is the error estimator, because that value is the inverse of the constant in the upper bound for the discretization error. Here, our ratio is around 3, so our estimator can be considered quite satisfactory. On the right, the estimated and exact error in the energy norm for adaptive and uniform refinement are displayed. The slopes of the lines are the convergence rates computed before. Observe the much better error reduction for the adaptive algorithm.

5.2. A nonconvex sector. In our second example, we consider the problem

$$-\mathrm{div}\,\boldsymbol{\sigma} = \mathbf{0} \quad \text{in } \Omega$$

with Dirichlet boundary conditions computed from the exact solution, where

$$\Omega := \{(r\cos\theta, r\sin\theta) : 0 < r < 1, 0 < \theta < 7\pi/8\}\,.$$

As before, we set the Lamé–parameters $\lambda = 4.6$ and $\mu = 0.63$. The exact solution for this problem is

$$\boldsymbol{u}(r,\theta) = \begin{pmatrix} r^\alpha(-(1+A_\alpha)\sin(\alpha\theta) + \sin((\alpha-2)\theta)) \\ r^\alpha(-\cos(\alpha\theta) + \cos((\alpha-2)\theta)) \end{pmatrix}$$

with $A_\alpha = \frac{2(\lambda+3\mu)}{(\lambda+\mu)\alpha}$ and $\alpha = 0.5240860003$. It is the same solution as in subsection 5.1, but we have a different α because of the different opening angle of the domain.

Figure 5.3 shows the initial and refined meshes. The solution has a singularity at $(0,0)$, so the adaptively refined meshes are, as expected, much more refined in this area.

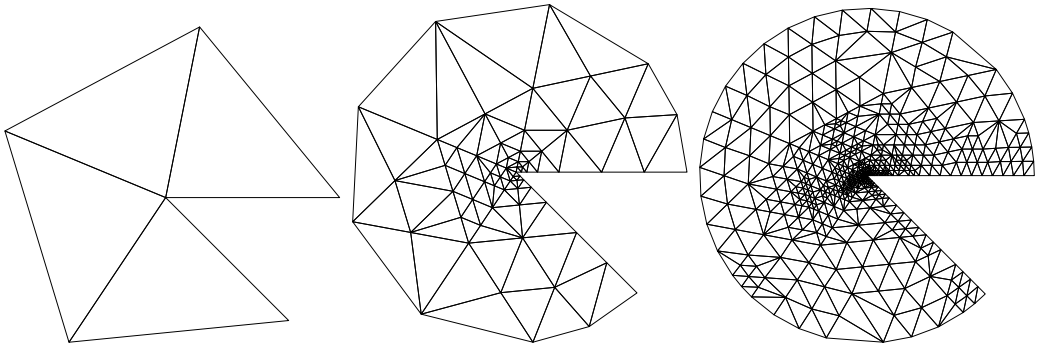

FIGURE 5.3. *Initial mesh (left) and adapted mesh after 5 (middle) and 10 (right) refinement steps for the example of subsection 5.2*

The averaged convergence rate s for the exact error using adaptive mesh refinement is 0.99967. For uniform refinement, the convergence rates tend to α.

Figure 5.4 shows the ratio between estimated and exact error and the estimated and exact error in the energy norm for uniform and adaptive refinement. As before, we remark that this ratio remains around a value between 2 and 4.

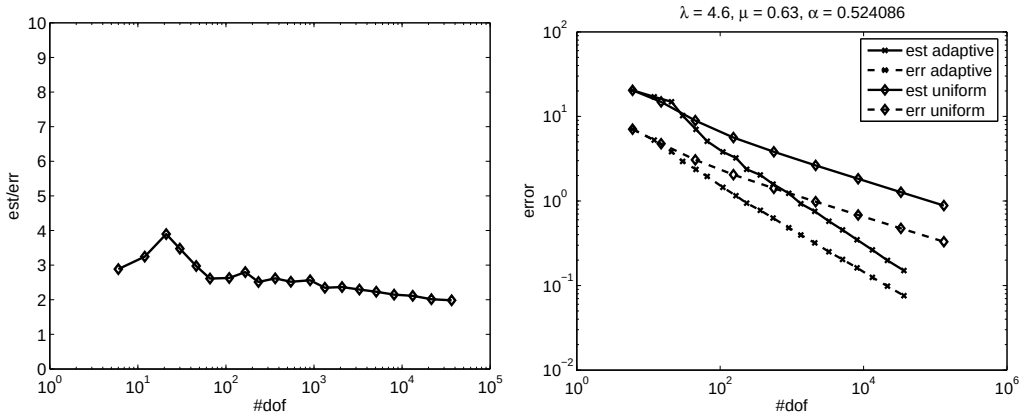

FIGURE 5.4. *Ratio between estimated and exact error (left) and error and error estimator for uniform and adaptive refinement (right) for the example of subsection 5.2*

5.3. Plate with hole under traction. In the last example, we consider a plate with a circular hole, subject to a shearing load on the right side, see [16].

Because of the symmetry, it is sufficient to consider only a quarter of the plate, if one enforces symmetry boundary conditions on the axis of symmetry of the entire plate, e.g. on the left homogeneous Dirichlet boundary conditions for the first component and homogeneous Neumann boundary conditions for the second component and below the other way around.

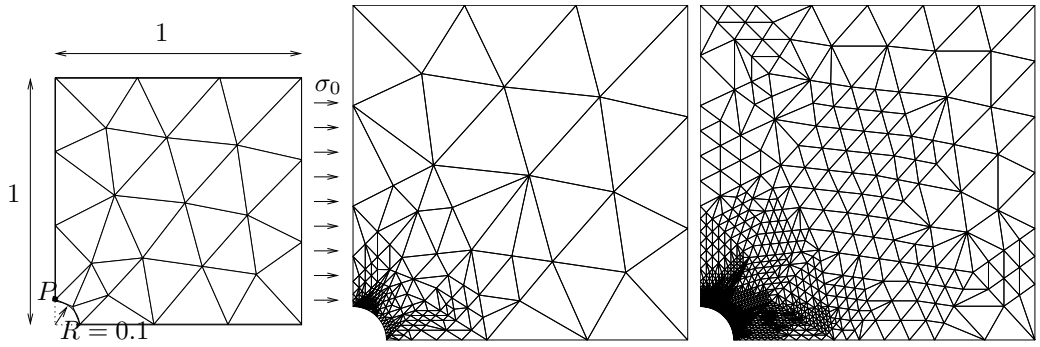

FIGURE 5.5. *Computational domain with initial mesh (left), adapted mesh after 5 (middle) and 10 (right) refinement steps for the example of subsection 5.3*

On the right, we have Neumann boundary conditions with $\boldsymbol{\sigma} \cdot \boldsymbol{n} = (\sigma_0, 0)^T$ and homogeneous Neumann boundary conditions elsewhere. For this example, we use $\sigma_0 = 1$, $E = 100000$ and $\nu = 0.3$. In Figure 5.5 the problem setting and initial mesh as well as adaptively refined meshes are depicted. As expected, the elements around the hole are much more refined, because the stress gradients are higher there.

In the case of an infinitely large, thin plate, a closed–form solution of this problem exists. Then the stress normal to the vertical plane of symmetry at point P (see Figure 5.5) is $\sigma_{xx} = 3\sigma_0$.

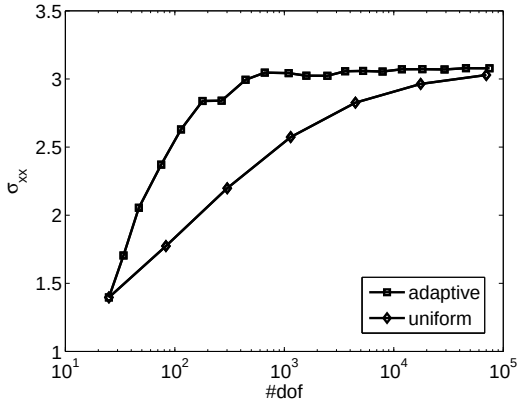

FIGURE 5.6. *σ_{xx} component of the stress tensor at point P for the example of subsection 5.3*

Figure 5.6 shows σ_{xx} as a function of the number of degrees of freedom for the adaptive and the uniform algorithm. In both cases, the value tends to the exact solution, but for the adaptive algorithm, we have a much faster convergence.

REFERENCES

[1] M. AINSWORTH AND I. BABUŠKA, *Reliable and robust a posteriori error estimation for singularly perturbed reaction-diffusion problems*, SIAM J. Numer. Anal., 36 (1998), pp. 331–353.

[2] M. AINSWORTH AND J. ODEN, *A posteriori error estimation in finite element analysis*, Chichester: Wiley, 2000.

[3] M. AINSWORTH AND J. T. ODEN, *A posteriori error estimators for 2nd order elliptic systems ii. an optimal order process for calculating self-equilibrated fluxes*, Comput. Math. Appl., 26 (1993), pp. 75–87.

[4] D. N. ARNOLD AND G. AWANOU, *Rectangular mixed finite elements for elasticity*, Math. Models Meth. Appl. Sci., 15 (2005), pp. 1417–1429.

[5] D. N. ARNOLD AND R. WINTHER, *Mixed finite element methods for elasticity*, Numer. Math., 92 (2002), pp. 401–419.

[6] ———, *Mixed finite elements for elasticity in the stress-displacement formulation*, in Current trends in sci-

entific computing, Z. Chen, R. Glowinski, and K. Li, eds., vol. 329 of Contemp. Math., Providence, RI, 2003, Amer. Math. Soc., pp. 33–42.

[7] I. Babuška, R. Duran, and R. Rodriguez, *Analysis of the efficiency of an a posteriori error estimator for linear triangular elements*, SIAM J. Numer. Anal., 29 (1992), pp. 947–964.

[8] I. Babuška and A. Miller, *A feedback finite element method with a posteriori error estimation. I: The finite element method and some basic properties of the a posteriori error estimator*, Comput. Methods Appl. Mech. Eng., 61 (1987), pp. 1–40.

[9] I. Babuška and W. Rheinboldt, *A posteriori error estimates for the finite element method*, Int. J. Numer. Methods Eng., 12 (1978), pp. 1597–1615.

[10] I. Babuška and T. Strouboulis, *The finite element methods and its reliability*, Oxford: Clarendon Press, 2001.

[11] R. Bank and A. Weiser, *Some a posteriori error estimates for elliptic partial differential equations*, Mathematics of Computation, 44 (1985), pp. 283–301.

[12] R. E. Bank and A. Weiser, *Some a-posteriori error estimators for elliptic partial differential equations*, Math. Comp., 44 (1990), pp. 283–301.

[13] S. C. Brenner and L. R. Scott, *The mathematical theory of finite element methods*, Springer, New York, 1994.

[14] F. Brezzi and M. Fortin, *Mixed and hybrid finite element methods*, Springer–Verlag, New York, 1991.

[15] U. Brink and E. Stein, *A posteriori error estimation in large-strain elasticity using equilibrated local neumann problems*, Comput. Methods Appl. Mech. Eng., 161 (1998), pp. 77–101.

[16] C. Carstensen, P. Causin, and R. Sacco, *A posteriori dual-mixed adaptive finite element error control for Lamé and Stokes equations*, Numer. Math., 101 (2005), pp. 309–332.

[17] P. G. Ciarlet, *The finite element method for elliptic problems*, North-Holland, Amsterdam, 1978.

[18] D. Kelly, *The self-equilibration of residuals and complementary a posteriori error estimates in the finite element method*, Int. J. Numer. Methods Eng., 20 (1984), pp. 1491–1506.

[19] D. Kelly and J. Isles, *Procedures for residual equilibration and local error estimation in the finite element method*, Commun. Appl. Numer. Methods, 5 (1989), pp. 497–505.

[20] P. Ladevèze, G. Coffignal, and J. P. Pelle, *Accuracy of elastoplatic and dynamic analysis*, Applied Numerical Mathematics, John Wiley & Sons, 1986.

[21] P. Ladevèze and D. Leguillon, *Error estimate procedure in the finite element method and applications*, SIAM J. Numer. Anal., 20 (1983), pp. 485–509.

[22] P. Ladevèze, J. P. Pelle, and P. Rougeot, *Error estimates and mesh optimization for finite element computation*, Engrg. Comp., 8 (1991), pp. 69–80.

[23] P. Ladevèze and P. Rougeot, *New advances on a posteriori error on constitutive relation in f.e. analysis*, Comput. Methods Appl. Mech. Eng., 150 (1997), pp. 239–249.

[24] R. Luce and B. Wohlmuth, *A local a posteriori error estimator based on equilibrated fluxes*, SIAM J. Numer. Anal., 42 (2004), pp. 1394–1414.

[25] S. Ohnimus, E. Stein, and E. Walhorn, *Local error estimates of FEM for displacements and stresses in linear elasticity by solving local Neumann problems*, Int. J. Numer.Meth. Engng., 52 (2001), pp. 727–746.

[26] E. Stein and S. Ohnimus, *Equilibrium method for postprocessing and error estimation in the finite element method*, Comput. Assist. Mech. Eng. Sci., 4 (1997), pp. 645–666.

[27] ———, *Anisotopic discretization- and model-error estimation in solid mechanics by local Neumann problems*, Comput. Methods Appl Mech. Engrg., 176 (1999), pp. 363–385.

[28] E. Stein, S. Ohnimus, and E. Walhorn, *Adaptive finite element discretization in eleasticity and elastoplasticity by global and local error estimators using local Neumann–problems*, Zeitschrift f. Angewandte Mathematik und Mechanik, 79 (1999), pp. 147–150.

[29] R. Verfürth, *A review of a posteriori error estimation and adaptive mesh–refinement techniques*, Wiley–Teubner Series Advances in Numerical Mathematics, Wiley–Teubner, Chichester, Stuttgart, 1996.

[30] ———, *A review of a posteriori error estimation techniques for elasticity problems*, Comput. Methods Appl. Mech. Engrg., 176 (1999), pp. 419–440.

[31] Y. Wang, *Preconditioning for the mixed formulation of linear plane elasticity*, PhD thesis, Texas A & M University, 2004.

[32] J. Z. Zhu and O. C. Zienkiewicz, *Adaptive techniques in the finite element method*, Commun. Appl. Numer. Methods, 4 (1988), pp. 197–204.

[33] O. C. Zienkiewicz and J. Z. Zhu, *A simple error estimator and adaptive procedure for practical engineering analysis.*, Internat. J. Numer. Methods Engrg., 24 (1987), pp. 337–357.

Erschienene Preprints ab Nummer 2006/001

Komplette Liste: `http://preprints.ians.uni-stuttgart.de`

2006/001 *Klimke, A.:* Sparse Grid Interpolation Toolbox - User's Guide

2006/002 *Klimke, A., Wohlmuth, B.:* Constructing Dimension-Adaptive Sparse Grid Interpolants using Parallel Function Evaluations

2006/003 *Hartmann, S., Brunssen, S., Ramm, E., Wohlmuth, B.:* Application of a primal-dual active set strategy for unilateral non-linear dynamic contact problems of thin-walled structures

2006/004 *Sändig, A.-M.:* Partielle Differentialgleichungen Vorlesung im Wintersemester 2005/2006

2006/005 *Nicaise, S., Witowski, K., Wohlmuth, B.:* An a posteriori error estimator for the Lame equation based on H(div)-conforming stress approximations